Nanosheets

DOI: 10.1002/anie.201004053

Janus Nanomembranes: A Generic Platform for Chemistry in Two Dimensions**

*Zhikun Zheng, Christoph T. Nottbohm, Andrey Turchanin, Heiko Muzik, André Beyer, Mike Heilemann, Markus Sauer, and Armin Gölzhäuser**

Chemistry in two dimensions differs significantly from chemistry in three-dimensional gases, liquids, or solids. A prominent example is heterogeneous catalysis, where the presence of two-dimensional (2D) surfaces can dramatically change the kinetics of a chemical reaction. Surfaces form at the limiting boundaries of a solid or a liquid. They are an integral part of condensed matter, and a surface rests on a bulk that provides it with structural integrity. Simply speaking, there is no surface without a bulk. However, recently extremely thin (<2 nm) but mechanically stable, free-standing, and self-supporting 2D materials have been described[1,2] that are practically surfaces without bulk. These nanomaterials, such as 2D polymers, nanosheets, and nanomembranes are free-standing in vacuum, gases, or liquids. They can even be transported from one environment to another without losing their structural intensity. 2D nanomaterials provide new opportunities for 2D chemistry and physics and also for applications. A bifacial Janus nanomembrane[3] in which both sides carry different chemical functions would provide a generic platform for directional chemistry. Such a system would be useful for nanoscale 2D sensors or actuators[4–6] in which the sides of a Janus nanomembrane specifically and independently detect atoms or molecules.[7–9] Differently functionalized surfaces are also driving forces for transport across nanomembranes, in a similar fashion to proton, electron, or ion pumps in biological systems.[10–12] An asymmetric functionalization further enables materials separation, as interactions with the functionalized surfaces[13] can advance the separation with molecular-level control.[14] However, despite many desirable uses, functional self-supporting 2D nanosystems are scarce, and in a recent review it was pointed out that "*making 2D polymers […] is still a dream of many organic and polymer chemists*".[5] To build free-standing membranes with a thickness less than 2 nm, different strategies, namely mechanical exfoliation,[1] layer-by-layer assembly,[15] or two-dimensional polymerization[16] have been explored.

Herein, we present an approach to fabricate a 1 nm thick Janus membrane by converting a surface-supported monomolecular film into a self-supported nanomembrane. We start by forming a self-assembled monolayer (SAM) on a solid surface. SAMs are well-ordered 2D molecular assemblies that are formed by chemical adsorption of amphiphilic molecules onto the surface of solids.[17,18] As the constituting molecules adsorb directionally, SAMs are also bifacial. However, one of the two faces of a SAM, the head group, is bound to the solid surface and is not available for chemical reactions, and a SAM therefore only interacts with its tail groups. It has been shown[2,6,19,20] that aromatic SAMs are dehydrogenated and laterally cross-linked into 2D nanosheets by exposure to electrons or UV light. In SAMs of aromatic units terminated by nitro groups, the hydrogen released during this process reduces the nitro groups to amino groups.[21,22] This process enables the immobilization of other molecules onto the cross-linked SAM by covalent coupling to the amino groups.[23–26] Recently, it was shown that cross-linked SAMs can be released from surfaces, forming 1 nm thick free-standing 2D nanosheets that are mechanically and chemically stable.[2,27,28] When a cross-linked thiol SAM is released, its sulfur head groups are no longer bound to a surface and can act as anchors to immobilize specific molecules on their side of the nanosheet. The liberation of the head groups opens the opportunity to make a 1 nm thick bifacial Janus nanomembrane with one amino and one thiol side (Scheme 1 a) that can immobilize different molecules on either side.

To fabricate the Janus nanomembrane, we self-assembled 4′-nitro-1,1′-biphenyl-4-thiol (NBPT) on a gold surface and exposed the SAM to electrons (100 eV, 50 mC cm^{-2}) to cross-link it into an approximately 1 nm thick sheet with amino and thiol sides. After the nanosheet is released from the surface, each side was functionalized with a different fluorescent dye, which can be easily detected by fluorescence microscopy. The amino groups on one side are modified with tetramethylrhodamine isothiocyanate (TMR), and the thiol groups on the other side with ATTO647N maleimide (Scheme 1 b). To confirm the immobilization of molecules on the nanomembranes, we employed X-ray photoelectron spectroscopy (XPS), scanning electron microscopy (SEM), and fluorescence microscopy. Fluorescence resonance energy transfer (FRET) from the donor TMR to the acceptor ATTO647N will show that both dyes are immobilized on different sides of

[*] Dr. Z. Zheng, Dr. C. T. Nottbohm, Priv.-Doz. Dr. A. Turchanin, H. Muzik, Priv.-Doz. Dr. A. Beyer, Dr. M. Heilemann, Prof. Dr. A. Gölzhäuser
Fakultät für Physik, Universität Bielefeld
33615 Bielefeld (Germany)
E-mail: ag@uni-bielefeld.de
Homepage: http://www.physik.uni-bielefeld.de/pss
Prof. Dr. M. Sauer
Biotechnology & Biophysics
Julius-Maximilians-University Würzburg
97074 Würzburg (Germany)

[**] We thank the Volkswagenstiftung and the Deutsche Forschungsgemeinschaft (SFB 613) for financial support. This work partly results from participation in the COST Action CM0601, "Electron Controlled Chemical Lithography" (ECCL). We thank Matthias Büenfeld, Tobias Klamp, and Mark Schnietz for their assistance with experimental setups.

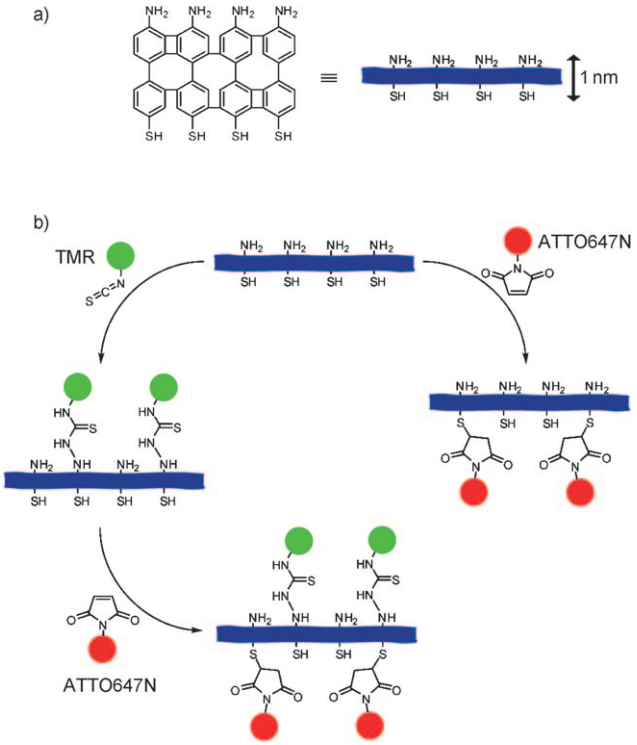

Scheme 1. a) A nanomembrane made from cross-linked biphenyl self-assembled monolayers. The 1 nm thick membrane has amino and thiol functional groups on its upper and lower sides, respectively. b) Functionalization with fluorescent dyes of the upper and lower sides of the nanomembranes. The amino side is functionalized with TMR, the thiol side with ATTO647N.

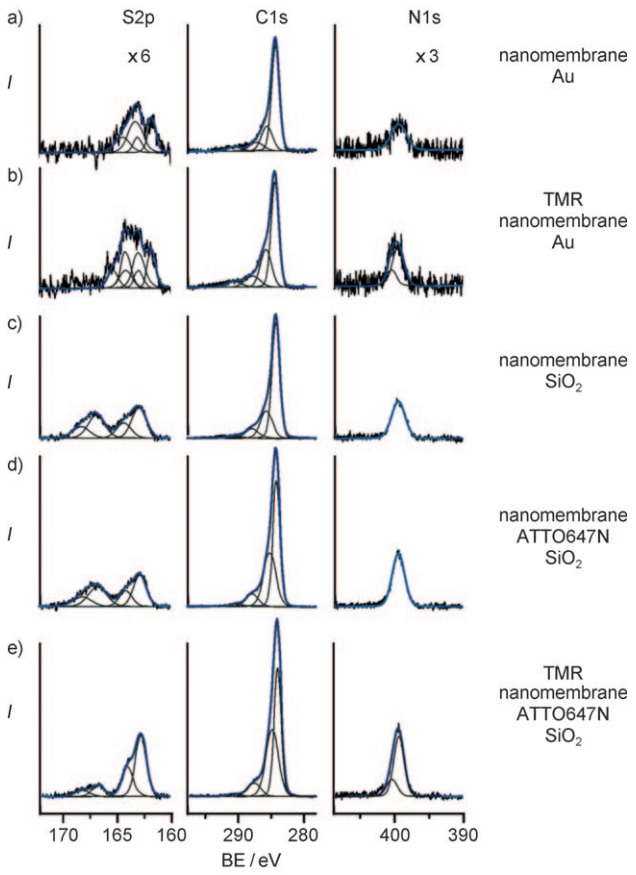

Figure 1. X-ray photoelectron spectra showing the selective functionalization of nanomembranes. a) Electron cross-linked NBPT SAM (50 mC cm^{-2}, 100 eV) on gold. b) Nanomembrane functionalized with TMR by amino groups. c) Nanomembrane transferred onto silicon oxide. d) Nanomembrane functionalized with ATTO647N by thiol groups and transferred onto silicon oxide. e) Janus nanomembrane functionalized on its upper side with TMR and on its lower side with ATTO647N, transferred onto silicon oxide. The S 2p and N 1s spectra were expanded by a factor of 6 and 3, respectively. The signal-to-noise ratio for gold surfaces is higher than for silicon oxide substrates owing to different secondary electron yields.

an ultrathin membrane.[29] Figure 1 a shows XP spectra of S 2p, C 1s, and N 1s signals[21,25] from a cross-linked NBPT SAM on gold. The S 2p signal consists of two atomic species with S $2p_{3/2}$ binding energies (BEs) of 162.0 and 163.5 eV that are due to thiolates and sulfides/disulfides formed upon irradiation, respectively.[20] The C 1s signal consists of peaks at 284.2 eV and 285.3 eV, which are assigned to aromatic carbon and to C–S and C–N bonds, respectively; furthermore, aromatic shake-up satellites are observed at 287–290 eV.[25] The N 1s signal at about 399 eV is characteristic for amino groups.[21] Figure 1 b shows XP spectra after the binding of TMR. The sulfur spectrum indicates the presence of a new species at a S $2p_{3/2}$ BE of about 164 eV, which is assigned to sulfur in TMR. The intensity of the C 1s signal increases by about 20 % owing to a new peak at about 285.3 eV. In the N 1s spectrum, a new species at about 400 eV is assigned to nitrogen in TMR. From the attenuation of the Au $4f_{7/2}$ signal (not shown), an increase of the effective thickness by 0.3 nm is calculated, which confirms a coupling of TMR to the amino side of the nanomembrane.

To test its functionality, the nanomembrane was transferred from the gold surface onto a copper transmission electron microscopy (TEM) grid by a procedure described in Ref. [28]. Figure 2 a,b shows fluorescence microscopy and SEM images of a TMR-

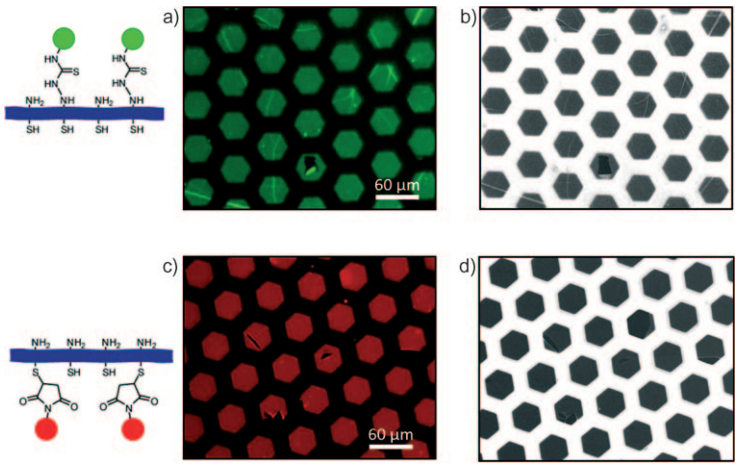

Figure 2. Diagrams and fluorescence micrographs of nanomembranes freely suspended over TEM grids. a) Amino side functionalized with TMR and c) thiol side functionalized with ATTO647. The corresponding SEM micrographs in (b) and (d) show the same pieces of nanomembrane as (a) and (c), respectively.

labeled nanomembrane suspended over a TEM grid. The homogeneity of the fluorescence indicates a uniform density of dyes coupled to the amino side. The bright lines in Figure 2a indicate folds in the membrane; in one comb the membrane is ruptured, as can be seen in the SEM image (Figure 2b). The parts of the membrane in contact with the honeycomb copper grid show no fluorescence because of non-radiative energy transfer to the metal.

To immobilize ATTO647N on the thiol side of the nanomembrane (Scheme 1b), the membrane is released from the surface by dissolving the gold. As the etching solution may have oxidized the sulfur at the lower side, we conducted a reductive treatment with sodium borohydride to create thiol groups. These groups can be used as anchors for the conjugation of ATTO647N functionalized with maleimide groups (Scheme 1b). Figure 1c shows XP spectra of a nanosheet that was transferred onto silicon oxide. The C1s and N1s signals are similar to those on the gold surface (Figure 1a). The S2$p_{3/2}$ signal at 163.2 eV is assigned to unbound thiol[30] that forms after the reduction with sodium borohydride. Its BE overlaps with the sulfur species formed upon electron irradiation.[20,30] A signal at 167.5 eV indicates the formation of some highly oxidized sulfur.

The XP spectra in Figure 1d demonstrate the coupling of ATTO647N to the thiol group of a nanosheet by an increase of the C1s and N1s intensities (compared to Figure 1c) and by a 0.5 nm increase of the effective thickness. The thickness was calculated from the attenuation of the Si2p signal (not shown). The conjugation of ATTO647N to the thiol side of the nanomembrane proceeds mostly by reaction of maleimide to thiol groups and also partly by electrostatic interactions. As ATTO647N maleimide is a cationic fluorophore with a net electrical charge of +1, it is electrostatically attracted to the oxidized sulfur species (BE = 167.5 eV), as they possess a net negative charge in water. This assumption is supported by the fact that the coupling of ATTO647N to the lower side was possible without sodium borohydride treatment; that is, formation of thiol groups. However, as shown by XPS and fluorescence microscopy, this electrostatic coupling was less efficient than maleimide coupling to thiols.

Figure 2c,d shows fluorescence micrographs and SEM images of a nanomembrane functionalized on its thiol side with ATTO647N. The fluorophore coverage is homogeneous over the entire membrane. Similar to the functionalization of the amino side with TMR (Figure 2a,b) intact, folded or ruptured areas are clearly recognized.

Finally, we fabricated Janus nanomembranes by the functionalization of both sides (Scheme 1b). We first immobilized TMR on the amino side and then coupled ATTO647N to the thiol side. Figure 1e shows XP spectra of a bifacial nanomembrane that has been transferred onto a silicon oxide substrate. The sulfur, carbon, and nitrogen signals appear to be a superposition of Figure 1b,d, as would be expected for a membrane with TMR and ATTO647N, thus indicating a successful functionalization of both sides. The thickness of the membrane without dyes is about 1 nm, thus we can expect an efficient FRET[29] between the dyes immobilized on both sides. Figure 3 shows fluorescence images of a) TMR, b) ATTO647N, c) FRET between TMR and ATTO647N, and d) a SEM image of the same area. Similar to the results in Figure 2, the functionalization with the fluorophores, as well as folds and ruptures are observable in all of the micrographs. However, the fluorescence intensity of TMR is much lower than in Figure 2a owing to efficient FRET to ATTO647N, a fact further corroborated by the FRET signal shown in Figure 3c. The FRET efficiency was determined to be effectively 100%, as expected for two fluorophores separated by a distance of about 1 nm, which is much shorter than the Förster radius.[29] In the SEM micrograph of Figure 3d, some ruptures in the membrane widened compared to the fluorescence images (Figure 3a–c). This effect most likely occurred during the transport from the fluorescence microscope into the electron microscope. Figure 4a shows a SEM image of a grid covered by single- and double-layer nanomembranes together with a diagram of the spatial arrangement. Double

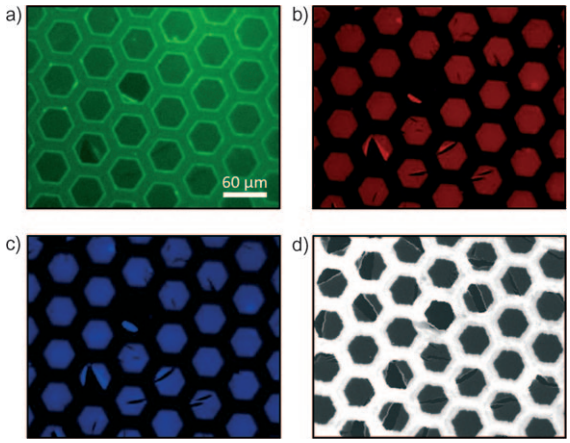

Figure 3. a, b) Fluorescence and c) FRET images, and d) the corresponding SEM image of a nanomembrane functionalized on its upper and lower sides with TMR and ATTO647N, respectively. The FRET image has been recorded by exciting at the donor wavelength and recording the fluorescence emission in the acceptor channel. All micrographs show the same area of the nanomembrane.

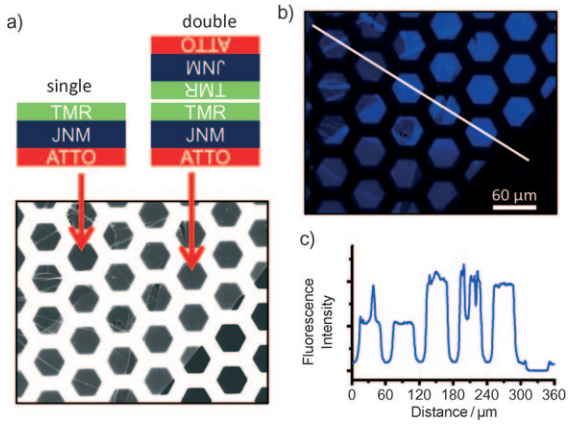

Figure 4. a) SEM image of a nanomembrane with areas of single and double layers. b) FRET image of the same area of the nanomembrane. c) Line profile showing different levels in fluorescence intensity corresponding to regions with single, double, and no nanomembrane, as indicated in (a).

layers are formed by a controlled placement of one piece of nanomembrane onto another (see Experimental Section). Figure 4b shows a FRET intensity image of the same nanomembrane, recorded by exciting the donor fluorophore TMR and detecting the fluorescence of the acceptor fluorophore ATTO647N. The image contains regions with free-standing single and double layers. The line profile (Figure 4c) shows the acceptor fluorescence intensity measured by FRET, and regions with one layer, two layers, or without membrane are clearly distinguished by their respective intensity levels. Together with XPS data, the observation of a strong and homogeneous FRET signal is an unequivocal evidence for the close proximity of the two dyes at antagonistic sides of the membrane and thus of the fabrication of a functional Janus nanomembrane.

In summary, we have shown the selective chemical functionalization of free-standing nanomembrane with distinct and different chemical functionalities (amino and thiol groups) on its sides. This sheet, which is only 1 nm thick, is modified into a true two-dimensional bifacial Janus system as each side is coated with different fluorescent dyes (TMR and ATTO647N). As there is only 1 nm separation between the dyes, an effective fluorescence energy transfer takes place, thus demonstrating the function of the Janus membranes as a platform for two-dimensional chemistry. The route to the fabrication of Janus membranes is universal and can be utilized for the immobilization of a variety of molecules. Therefore, two-dimensional devices with various functionalities become conceivable as an effective control over chemical modifications of the Janus membrane can now easily be achieved.

Experimental Section

4′-nitro-1,1′-biphenyl-4-thiol (NBPT) (Taros, 95%) was purified by sublimation. *N*,*N*-dimethylformamide (DMF) (p.a., VWR) was dried over 4 Å molecular sieves. All other chemicals were used as received.

Fabrication of nanomembranes: Mica substrates with 300 nm thermally evaporated Au (Georg Albert PVD) were cleaned in an UV/ozone cleaner (FHR), rinsed with ethanol, and blown dry in N_2. They were then immersed in a circa 1 mmol L^{-1} solution of NBPT in dry and degassed DMF for three days in a sealed flask under N_2. The samples were rinsed with DMF, ethanol, and dried in a N_2 stream. Cross-linking was performed in high vacuum ($< 5 \times 10^{-7}$ mbar) with an electron floodgun (Specs FG20) at an energy of 100 eV and a dose of 50 mC cm^{-2}.

Functionalization of the amino side: Tetramethylrhodamine (TMR) isothiocyanate (0.2 μmol, Sigma–Aldrich) was dissolved in dry DMF (10 μL) and then diluted with a sodium bicarbonate buffer (0.1 mol L^{-1}, 1 mL; Sigma–Aldrich). The nanomembrane on Au/mica was immersed in this solution for about 3 h. Thereafter, the sample was washed with methanol and water and dried in N_2.

Functionalization of the thiol side: Sodium borohydride (2 mmol; 98%, Sigma–Aldrich) was dissolved in a sodium hydroxide (VWR) aqueous solution (0.1 mol L^{-1}, 10 mL). Polymethylmethacrylate (PMMA; Allresist)-stabilized nanomembrane was then allowed to float on this solution for about 1 hour, rinsed with degassed Milli-Q water, and then transferred to ATTO647N maleimide (0.1 mmol L^{-1}, Attotec) in HEPES buffer solution (10 mmol L^{-1}, pH 7.2; Sigma-Aldrich) for about 2 h under N_2. Thereafter, the sample was suspended on water for at least 12 h before it was transferred to its substrate.

Transfer of nanomembrane was achieved by stabilizing the membrane with a spin-coated layer of PMMA. The Au was then cleaved from the mica by immersion in hydrofluoric acid for 5 min and etched in an I_2/KI-etch bath (ca. 15 min). Thereafter the PMMA/nanomembrane (modified or unmodified) was transferred to its substrate followed by dissolution of the PMMA in acetone to yield a clean membrane.

Free-standing double layers: A TMR/nanomembrane/Au sandwich protected by a circa 300 nm thick photoresist was released from a mica substrate, immersed in acetone to remove the photoresist, and then placed onto a TMR/nanomembrane/ATTO647N on a Si_3N_4 substrate. The gold was removed by an I_2/KI etch, and the freshly exposed sulfur side was modified with ATTO647N maleimide. Transfer to TEM grids was conducted as described above. For sample drying, a critical-point dryer was used (Tousimis Autosamdri).

X-Ray photoelectron spectroscopy was carried out in ultrahigh vacuum (ca. 10^{-10} mbar) in an Omicron spectrometer with a monochromatic X-ray ($Al_{K\alpha}$)) source. Binding energies are referred to the Au $4f_{7/2}$ peak at 84.0 eV for the samples on gold, or to the main peak of the C 1s signal at 284.2 eV for samples transferred onto SiO_2. Thickness calculations were based on attenuation of the substrate Au $4f_{7/2}$ ($\lambda = 36$ Å) or Si 2p ($\lambda = 35$ Å) signals. For peak fitting, a Shirley background and symmetric Voigt functions were used. The separation between S $2p_{3/2}$ and S $2p_{1/2}$ was taken to be 1.2 eV.

Fluorescence microscopy was performed on an inverted microscope (Olympus IX 71) equipped with a Hg lamp and operated in wide-field illumination. The excitation wavelength was selected by appropriate band-pass filters (480BP20 for TMR, 630BP10 for ATTO647N; AHF Analysentechnik). The excitation light was directed using a dichroic beamsplitter (488/640 dual band; AHF) through an air objective (10×, NA 0.30, Olympus). Fluorescence emission was collected through the same objective and separated from the excitation by dichroic beam splitters and band pass filters (580DF60 for TMR, 700DF75 for ATTO647N; AHF). An electron-multiplying charge-coupled device (Picostar, LaVision) was used to record fluorescence images. Scanning electron microscopy (SEM) images were obtained with an Multiscan system (Omicron/Zeiss) at an energy of 3 kV.

Received: July 2, 2010
Published online: September 30, 2010

Keywords: fluorescent dyes · Janus membranes · monolayers · nanosheets · polymerization

[1] K. S. Novoselov, D. Jiang, F. Schedin, T. J. Booth, V. V. Khotkevich, S. V. Morozov, A. K. Geim, *Proc. Natl. Acad. Sci. USA* **2005**, *102*, 10451.
[2] W. Eck, A. Küller, M. Grunze, B. Völkel, A. Gölzhäuser, *Adv. Mater.* **2005**, *17*, 2583.
[3] Janus is a Roman god with two faces. The term "Janus" is also used to describe particles that have different surfaces on opposite sides.
[4] C. Y. Jiang, S. Markutsya, Y. Pikus, V. V. Tsukruk, *Nat. Mater.* **2004**, *3*, 721.
[5] J. Sakamoto, J. van Heijst, O. Lukin, A. D. Schlüter, *Angew. Chem.* **2009**, *121*, 1048; *Angew. Chem. Int. Ed.* **2009**, *48*, 1030.
[6] M. Schnietz, A. Turchanin, C. T. Nottbohm, A. Beyer, H. H. Solak, P. Hinze, T. Weimann, A. Gölzhauser, *Small* **2009**, *5*, 2651.
[7] J. R. Barnes, R. J. Stephenson, M. E. Welland, C. Gerber, J. K. Gimzewski, *Nature* **1994**, *372*, 79.
[8] J. Fritz, M. K. Baller, H. P. Lang, H. Rothuizen, P. Vettiger, E. Meyer, H. J. Guntherodt, C. Gerber, J. K. Gimzewski, *Science* **2000**, *288*, 316.
[9] P. S. Waggoner, H. G. Craighead, *Lab Chip* **2007**, *7*, 1238.
[10] R. D. Astumian, I. Derenyi, *Eur. Biophys. J.* **1998**, *27*, 474.

[11] S. Matthias, F. Müller, *Nature* **2003**, *424*, 53.
[12] I. Kosztin, K. Schulten, *Phys. Rev. Lett.* **2004**, *93*, 238102.
[13] M. Majumder, N. Chopra, B. J. Hinds, *J. Am. Chem. Soc.* **2005**, *127*, 9062.
[14] K. M. Lee, L. C. Li, L. M. Dai, *J. Am. Chem. Soc.* **2005**, *127*, 4122.
[15] D. Zimnitsky, V. V. Shevchenko, V. V. Tsukruk, *Langmuir* **2008**, *24*, 5996.
[16] M. J. Schultz, X. Zhang, S. Unarunotai, D.-Y. Khang, Q. Cao, C. Wang, C. Lei, S. MacLaren, J. A. N. T. Soares, I. Petrov, J. S. Moore, A. Rogers, *Proc. Natl. Acad. Sci. USA* **2008**, *105*, 7353.
[17] A. Ulman, *Thin Films: Self-assembled Monolayer of Thiols*, Academic Press, San Diego, **1998**.
[18] J. C. Love, L. A. Estroff, J. K. Kriebel, R. G. Nuzzo, G. M. Whitesides, *Chem. Rev.* **2005**, *105*, 1103.
[19] W. Geyer, V. Stadler, W. Eck, M. Zharnikov, A. Gölzhäuser, M. Grunze, *Appl. Phys. Lett.* **1999**, *75*, 2401.
[20] A. Turchanin, D. Käfer, M. El-Desawy, C. Wöll, G. Witte, A. Gölzhäuser, *Langmuir* **2009**, *25*, 7342.
[21] W. Eck, V. Stadler, W. Geyer, M. Zharnikov, A. Gölzhäuser, M. Grunze, *Adv. Mater.* **2000**, *12*, 805.
[22] A. Turchanin, M. Schnietz, M. El-Desawy, H. H. Solak, C. David, A. Gölzhäuser, *Small* **2007**, *3*, 2114.
[23] A. Biebricher, A. Paul, P. Tinnefeld, A. Gölzhäuser, M. Sauer, *J. Biotechnol.* **2004**, *112*, 97.
[24] U. Schmelmer, A. Paul, A. Küller, M. Steenackers, A. Ulman, M. Grunze, A. Gölzhäuser, R. Jordan, *Small* **2007**, *3*, 459.
[25] A. Turchanin, A. Tinazli, M. El-Desawy, H. Großmann, M. Schnietz, H. H. Solak, R. Tampé, A. Gölzhäuser, *Adv. Mater.* **2008**, *20*, 471.
[26] C. T. Nottbohm, R. Sopher, M. Heilemann, M. Sauer, A. Gölzhäuser, *J. Biotechnol.* **2010**, DOI: 10.1016/j.jbiotec. 2010.01.018.
[27] A. Turchanin, A. Beyer, C. T. Nottbohm, X. Zhang, R. Stosch, A. S. Sologubenko, J. Mayer, P. Hinze, T. Weimann, A. Gölzhäuser, *Adv. Mater.* **2009**, *21*, 1233.
[28] C. T. Nottbohm, A. Beyer, A. S. Sologubenko, I. Ennen, A. Hütten, H. Rösner, W. Eck, J. Mayer, G. A, *Ultramicroscopy* **2008**, *108*, 885.
[29] R. M. Clegg, *Curr. Opin. Biotechnol.* **1995**, *6*, 103.
[30] D. G. Castner, K. Hinds, D. W. Grainger, *Langmuir* **1996**, *12*, 5083.

